ANALYSIS OF AMBER SAMPLES BY LIBS AND CHEMOMETRICS METHODS

ANÁLISIS DE MUESTRAS DE ÁMBAR POR LIBS Y METODOS QUIMIOMETRÍCOS

T. Flores[a†], F. C. Alvira[b,c], A. Ponce[a], L. Ponce[a]

a) ONTEKO LLC, 9924 Alexander Ridge Dr., Olive Branch 38654, MS, USA; jesusehr@uclv.edu.cu[†]
b) Laboratorio de Bio-Nanotecnología Nacional de Quilmes Bernal, Departamento de Ciencia y Tecnología, Buenos Aires, Argentina
c) Grupo de Biología Estructural y Biotecnología (GBEyB), IMBICE (CONICET CCT-La Plata), Buenos Aires, Argentina
† corresponding author

We analyzed amber samples from the the Baltic region and Mexico, as well as imitation amber, in order to develop an analytical method allowing to discriminate between different samples causing little or no damage. We propose a two-step method that involves the use of Laser Induced Breakdown Spectroscopy (LIBS) to obtain spectra, and Discriminant Analysis to analyze the resulting data. We studied the damage caused to the samples using confocal optical microscopy.

En el presente trabajo se estudian muestras de ámbar del Baltico y de México, asi como ámbar de imitacion, con el objetivo de desarrollar un método analítico que permita discriminar entre diferentes muestras causando mínimo daño. Para optimizar la identificación se propone un método en tándem, utilizando la técnica LIBS para obtener los espectros, y el Análisis Discriminante para el tratamiento de los datos. Se estudia el daño causado a las muestras por microscopía óptica confocal.

I. INTRODUCTION

In addition to its intrinsic beauty, amber has been highly appreciated since ancient times, for its use in jewelry and the elaboration of objects of high artistic and decorative value. Amber is the oldest gemstone used in craftsmanship, with red amber being the most appreciated one [1].

In addition, amber is especially important because it commonly contains biological (microorganisms, plant, and animal remains) and non-biological inclusions (bubbles with gaseous, liquid, and sediment contents) that are conserved exceptionally well, showing delicate three-dimensional structures [2].

Amber from various regions can be found in the market: the main producers are the Baltic region, the Dominican Republic, and Mexico. Amber is characterized according to its color, transparency, and origin for commercial purposes. Unfortunately, there is also a wide assortment of amber replicas, based on various colored polymers. For commercial amber, the most common color is yellow, and the most expensive is red [3]. The rarest are those of cognac, green and blue tones. Some pieces contain fossil insects, trapped millions of years ago, being particularly valuable from a scientific point of view [1].

In Mexico, Chiapas is the only state in where amber can be found. Chiapas amber had a special meaning for Meso-American cultures, which used it to make ornaments and funeral offerings. For this reason, it was the subject of intense trade by the indigenous inhabitants of Chiapas, mainly Chontales, Tzotziles, and Zoques, and their destination was, mainly, the Aztec elite [4]. After the Spanish colonization, many of these museum pieces became part of private collections, while others are in public museums. Chiapas amber has the greatest variety of colors and hues, which is why it is the most appreciated worldwide [2,5].

Chiapas amber is the result of polymerization that occurred through millions of years of the resin produced by two species of legume tree, Hymenaea Mexicana and Hymenaea Allendi [6,7].

Although the amber of the Baltic region has been characterized in detail [8], the same does not occur in the case of amber from Chiapas or in that from the Dominican Republic.

The analytical methods used so far are expensive, destructive, or require time-consuming analysis. In 2003 Vandenabeele et al. [9] analized different Copal resins —a type of polymerized tree resin that hasn't been buried for long enough to fossilize into amber— from 6 regions of Mexico using Raman Spectroscopy (RS). They concluded that one of the ways to distinguish Copal depends on the presence of Calcium Carbonate (CaCO3). Other research groups have studied amber samples by RS. Brody et al [11] have studied amber by Fourier transform Raman Spectroscopy (FT-Raman spectroscopy). This is one of the most complex and expensive implementations of RS, where the detection system is a Michelson Interferometer. The authors of this research have also analyzed amber samples from several origins, including Mexico, the Baltic region, Poland, and the Dominican Republic. They have investigated the presence of diterpenoids and pimarane skeletons. They concluded that FT-Raman spectroscopy is useful to identify those diterpenoids, but they do not comment about the origin of the samples, nor an attempt of classification is done [12]. Chiang et al [13],

use RS to follow the maturation process of fossilized copal resins; they have used a standard Raman instrument, and in their spectra the fluorescence interference is appreciated. A. Schmidt et al. [14] conducted a thermogravimetric study to classify different types of amber. To determine the age of the resins, and in this way to know if it is amber or Copal, M. Feist et al. [15] in 2007, also performed thermogravimetric analysis. It has the disadvantage of being completely destructive to the sample, which makes its use unfeasible when it comes to the study of pieces of heritage value. Another technique used for the determination of amber origin is fluorescence spectroscopy. This is a non- destructive technique, but as was demonstrated by G. Lopez-Morales et al. [16], the study must be performed carefully, because if the samples are illuminated with a broad-spectrum source, this technique could fail to distinguish the true from the false amber. In addition to that, as the author mentions, glasses, resins and plastics can be easily doped with colorants and nano-particles, which could have similar fluorescent behavior as the true amber, making this technique vulnerable to falsifications.

Considering the variety of origin and diversity of shapes and colors, it is of great importance to have fast and effective methods to identify and characterize amber, both to avoid counterfeiting and to properly assign the heritage or scientific value of a sample.

Within the modern analytical techniques normally used in the characterization and conservation of objects of high added value, laser-induced plasma spectroscopy (LIBS) is increasingly used. LIBS is a type of atomic emission spectroscopy that uses high-energy laser excitation sources and is widely used for the compositional characterization of materials [16]. It has been shown in previous work that the spectra can be considered as a "fingerprint" of the sample material, effectively serving to differentiate between samples of very similar composition, revealing the most subtle differences thanks to the use of chemometric methods [13,17].

In this paper, we study the inorganic composition of amber employing laser-induced breakdown spectroscopy (LIBS) to quickly differentiate amber samples of various origins and colors. In particular, the study analyzed amber samples from Mexico, the Baltic region, as well as fake amber.

II. MATERIALS AND METHODS

II.1. LIBS set-up

For the analysis, we used a LIBS instrument, "SLIT-LIBS," supplied by Onteko LLC (Tampa, United States), which includes a laser that emits in a "burst mode" regime described below. In this device, the laser beam is coupled with the optical path of a slit-lamp microscope for better visualization of samples.

A schematic representation for this setup is shown in Fig. 1. The pulsed (neodymium: yttrium aluminum garnet) Nd:YAG laser emits at a wavelength of 1,064 nm while working in a Q-switch regime, producing light pulses (shots) with an energy of up to 40 mJ at a repetition rate of 1 Hz. A low-power

red laser was used to point where the Nd:YAG laser would impact and ablate the sample and generate the plasma. Each laser shot consisted of a train of three micro pulses, each having a duration of 8 ns and an interval of 10–25 μs between them, resulting in an overall shot duration of about 70–80 μs. To improve the detection limits, lasers are used in the multi-pulse mode for which each laser shot generates a pulse train (for a detailed description of those lasers, see ref. [14,18]). Thanks to a time-delay device, the spectrometer starts reading the signal 2 μs after the laser impacts the sample, providing sufficient time to avoid the capture of undesirable emissions from the electrons in the plasma of the first pulse, which, as is widely known, does not provide elementary information and has a lifetime of about 500 ns.
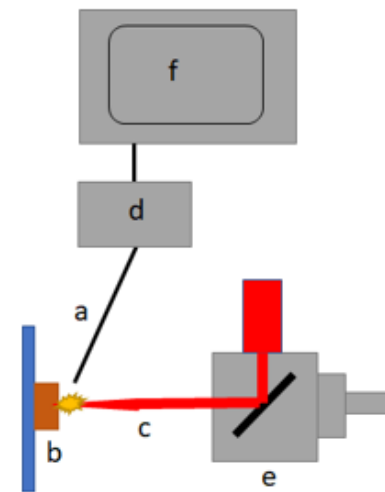
Figure 1. LIBS experimental set-up: a- detector, b- sample, c- laser beam, d- spectrometer, e- microscope, f -computer.

Since each acquired signal is the result of the sum of the three pulses, this setup can indeed remove only the electronic noise caused by the first pulse. As the spectrometer acquisition time is 3.8 ms long, both the signal and electronic noise from the subsequent pulses are also captured. The reduction of the Bremsthralung is related to the fact that all the samples have a thin layer of dirt. So, the first pulse makes a kind of "laser cleaning", and the second and third pulses find a clean surface to ablate. Since the radiation of the electrons generated during the first pulse is avoided, this improves the quality of the signal spectra. But as our experimental results show, the signal to noise ratio is good enough to provide a clear and intense signal.

The laser beam was focalized using a 50 mm focal length lens which produced a 40 μm diameter target on the samples. The laser ablation process induced the emission of light which was collected by an optical fiber and delivered to a Czerny–Turner spectrometer (OceanOptics USB4000) with a linear CCD as a detector. The spectral resolution of the system is 0.3 nm with a spectral range of 200–800 nm.

Next, the acquisition, storage, and analysis of the plasma spectral data acquired by the spectrometer are carried out. This information is supplied to a laptop using a USB port,

where the information is processed using the spectrometer software to visualize the plasma intensity profile as a function of wavelength. Also, the laptop can be programmed to identify the elementary composition of the sample through comparative analysis with known spectral profiles that are stored either on the computer or accessed, for example, through an internet link to a remote database.

II.2. Confocal microscopy

To observe the morphology and dimensions of the crater that occurs when a laser pulse strikes the sample, a confocal laser scanning microscope Olympus Model OLS5000 3D Measuring Laser Microscope was used.

II.3. Samples

The samples under study can be categorized into three groups. The first group consists of Mexican amber samples of two shades: Honey amber and Yellow amber. These samples were supplied and certified by the amber museum of Chiapas (group 1). The second group consists of certified Baltic samples with two different shades: honey amber cognac and yellow amber (group 2). The third group consists of replicas made of plastics, imitating the colors honey and yellow. They are of Chinese origin and acquired in the Amazon online store (group 3). We will call them "fake amber". See Table 3 for more details.

All the samples were prepared as pieces of 1 x 1 cm and 1 mm thickness and were polished. The sample area was enough to accommodate 50 laser pulses, each of them removing material from a 0.1 mm diameter spot.

II.4. Statistical analysis

The data was processed mathematically to be able to make groups according to their differences. In order to achieve this, all the spectral data were normalized with a maximum value of 1 for each spectrum. Due to the high resolution of the spectrometer, each spectra capture file is composed of 3648 wavelengths with their corresponding intensities. The size of these datasets implied a cumbersome processing, so they were downscaled from 3648 spectral channels to 174 by averaging segments of 20 channels into a single value. From this reduced dataset, the 20 points of the spectrum with the highest standard deviation for each amber category were selected as variables for a Discriminant Analysis (DA) [19]. After an initial approach with Linear Discriminant Analysis, a Box test indicated that the covariance matrix differed between some of the groups, so Quadratic Discriminant Analysis was used instead.

III. RESULTS AND DISCUSSIONS

III.1. LIBS Experiments

Each LIBS spectrum shown in Fig. 2, which corresponds to the different shades, is the average of 50 evaluations performed per sample. In the LIBS analysis of the Chiapas amber samples, we identify the presence of Na, Al, Ca, Sr, Fe, Cr, Mg, Ni, Cl, in addition to H, N, and CN bands. The last ones are associated with the air atmosphere. We found that the yellow samples do not show Fe emission lines, while for the rest of them, the main differences are in the intensities of the emission lines. Moreover, the darker samples have a lower intensity of Na and Al relative to the light ones. The opposite occurs for the Ca emission lines, that are higher in the lighter samples. In the Baltic amber as well as in the false amber, no Ca emission lines are visible, but Fe and Mg emission lines are appreciated. In the case of false amber, the 611.4 nm Cl line is always present.

Table 1. Samples description.

Groups	Origin	Shade	Number of samples	Spectra per sample
I	Chiapas	Honey	5	50
		Yellow	5	50
II	Baltic	Honey	5	50
		Yellow	5	50
III	FALSE	Honey	5	50
		Yellow	5	50

These spectral differences can be used to perform DA analysis and identify spectral differences between similar sample types with minor impurities.
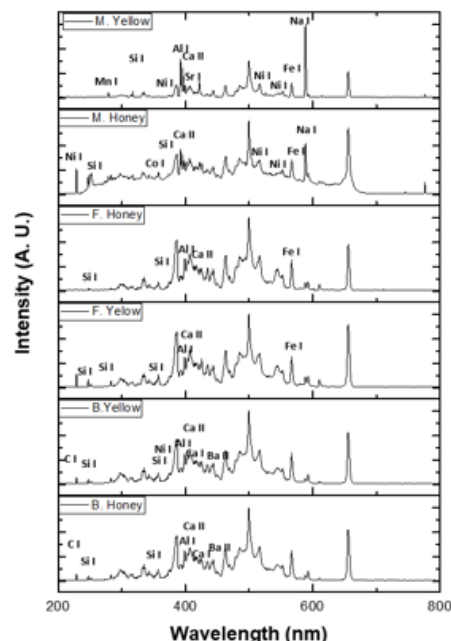
Figure 2. Average LIBS Spectra of all the samples under study.

III.2. Confocal Microscopy

To get an accurate knowledge of the damage caused in the samples to get the information, we studied the ablation effects by Confocal Microscopy. Fig. 3 shows an image captured by the confocal microscope, showing a cone-like crater.
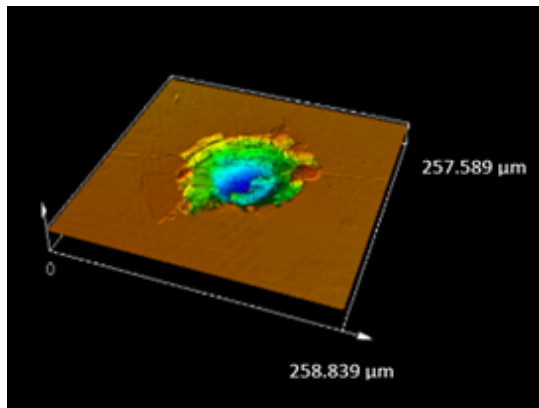
Figure 3. Crater image captured by Confocal Microscope at 50X magnification.

The laser pulse, upon impact on the surface, extracts the material from the first tens of microns, involving a very small volume of material. The volume extracted was calculated by approximating the geometry of the crater to a truncated cone with an upper radius of 58.5 μm and a lower radius of 16.0 μm, the measured height being 42.2 μm. The resulting volume was calculated as approximately 179 μm^3. These dimensions are below what is usually possible to see with the naked eye, which further supports the idea that LIBS could be used to detect the origin of valuable amber pieces without diminishing their value.

In some areas of the surface adjacent to the crater, defects are observed that could have been induced by the pressure generated below the surface due to the penetration of the laser into a relatively transparent material such as amber. Fig. 4 shows a sub-surface crater in the sample and the associated LIBS spectrum obtained. Let us compare those results with standard methods employed to acquire the same information.
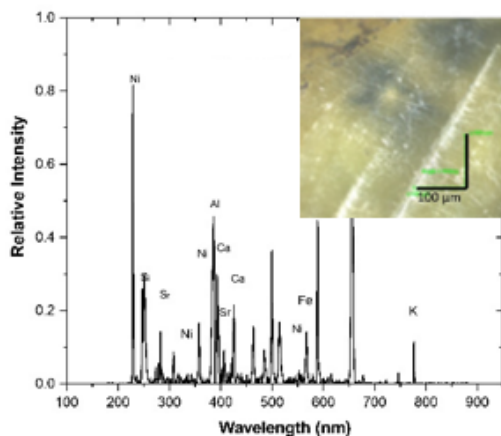
Figure 4. LIBS spectrum of a subsurface crater. Inset: sample region where the spectrum was acquired.

We underline that the standard atomic emission methods require the extraction of a tiny portion of the sample, and the dissolution in the acid of this portion. So, the damage generated by LIBS compared with standard analysis techniques is negligible.

III.3. Chemometrics analysis
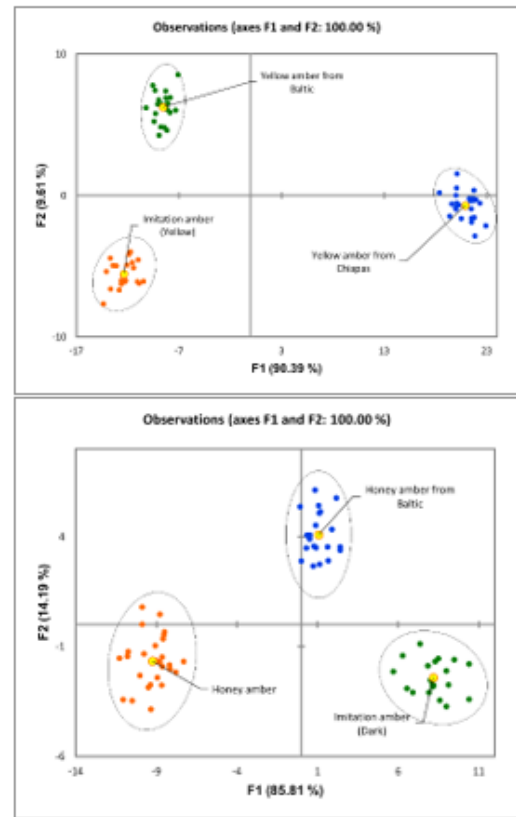
Figure 5. Differentiation between the various amber samples using Discriminant Analysis [19].

The identification of each type of amber is not evident by a straightforward study of the spectral information. In order to classify the samples, we analyzed the spectral data using Discriminant Analysis (DA) [19]. This is a classical statistical technique usually applied not only to LIBS analysis but to several other spectroscopic techniques. The algorithms used to implement DA can be implemented in standard personal computers. Thus, it seems to be an adequate candidate to process the spectral information to classify the amber samples. The algorithms successfully discriminated between different types of amber, as can be seen in Fig. 5. The most valuable result shown is the capacity of the LIBS-DA tandem techniques to differentiate the imitation samples of amber from original samples coming from the Baltic Sea and Chiapas. Fig. 6 (connected to the data presented in Table 2) presents a loading plot that provides valuable insights into the relationship between the 20 intensity variables selected and the two main functions in our discriminant analysis (DA). The plot shows how the variables contribute to the splitting into

two groups and helps identifying which variables are the most relevant for distinguishing between the groups. Specifically, the plot illustrates the correlation between each variable and the two main functions in the DA, with the magnitude and direction of each arrow representing the strength and direction of the correlation, respectively.
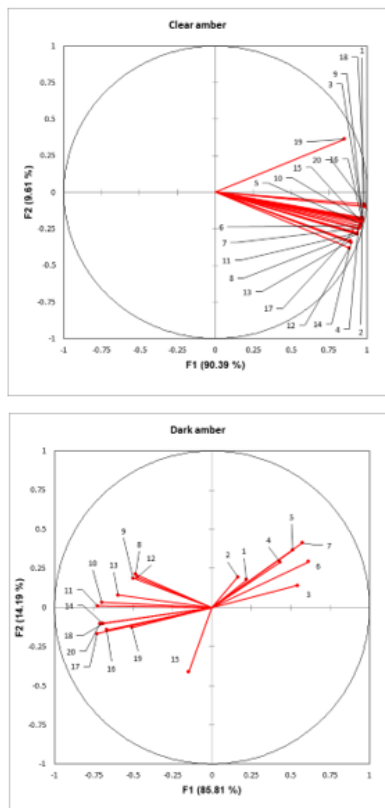
Figure 6. Loading plot detailing how the 20 intensity variables selected relate with the two main functions in the DA.

Table 2. Wavelengths of the intensity variables shown in Fig. 6.

Id.	Wavelength (nm)
1	383.9
2	388.3
3	405.5
4	490.5
5	494.7
6	498.9
7	503.1
8	528.1
9	532.2
10	557.0
11	561.1
12	565.2
13	569.3
14	573.4
15	589.6
16	593.7
17	649.8
18	653.7
19	657.7
20	661.6

We have shown that the LIBS technique can be used to obtain a general characterization of amber without causing excessive damage to the sample. By analyzing the main elements present in Chiapas amber, we were able to identify markers that can be used in a statistical system to determine authenticity, which is consistent with the type of soil found in the Simojovel mining area were the Chiapas samples were extracted. These elements include Na, Mg, Al, Si, K, Ca, Fe, Co, Ni, Mg, and Mn. Through the selection of specific spectral regions for these main elements and the use of different colors to represent each group, we were able to clearly distinguish between different types of amber based on their composition.

IV. CONCLUSIONS

Our results show that the use of LIBS with DA treatment for spectral analysis allows for accurate and rapid identification and discrimination of Mexican amber, Baltic amber, and false amber. The chemometrics techniques used in this study were found to be an effective and reliable tool for analyzing complex organic samples. Moreover, without any prior knowledge of the concentration of inorganic elements or other information about the samples, the proposed technique was able to accurately classify the samples based solely on the LIBS spectra. Overall, our results demonstrate the usefulness of the LIBS technique paired with multivariate analysis for the analysis and classification of amber samples.

ACKNOWLEDGMENTS

REFERENCES

[1] J. C. Cruz-Ocampo, C. Canet, D. Peña-García, Boletín Soc. Geol. Mexicana **59**, 9 (2007).
[2] E.Y.T. DE PRUEBA, PROYECTO de Norma Oficial Mexicana PROY-NOM-152-SCFI-2018, Ámbar de Chiapas-Especificaciones y métodos de prueba (cancelará a la NOM-152-SCFI-2003).
[3] F. P. Zepeda, Cadena productiva del ámbar en Chiapas, México, Lacandonia **3**, 69 (2017).
[4] C. Ytuarte-Núñez. Nueva antropología **22**, 11-31 (2009).
[5] T. P. Suárez, El ámbar en Chiapas y su distribuciçón en Mesoamçérica, Estudios de cultura maya **26**, 178 (2005), Recuperado en 09 julio de 2023 de http://www.scielo.org.mx/scielo.php?script=sci_arttext&pid=S0185-25742005000100010&lng=es&tlng=es
[6] L. Calvillo-Canadell, S.R. Cevallos-Ferriz, L. Rico-Arce, Rev. of Palaeobotany and Palynology **160**, 126 (2010).
[7] T. Pérez Suárez. Estudios de cultura maya **26**, 178 (2005).
[8] L. Aquilina, V. Girard, O. Henin, M. Bouhnik-Le Coz, D. Vilbert, V. Perrichot, D. Néraudeau, Palaeogeography, Palaeoclimatology, Palaeoecology **369**, 220 (2013).
[9] P. Vandenabeele, D.M. Grimaldi, H.G. Edwards, L. Moens, Spectrochim. Acta-A: Mol. Biomol. Spectrosc. **59**, 2221 (2003).

[10] Vicerrectorado de Investigaciones y Posgrado, UCLV, Reportes de aplicación 1985-1990.

[11] R. H. Brody, H. G. M. Edwards, A. M. Pollard, Spectrochim. Acta-A: Mol. Biomol. Spectrosc. **57**, 1325 (2001).

[12] G. Poinar Jr, A. E. Brown, Bot. J. of the Linnean Soc. **139**, 125 (2002).

[13] H. P. Chiang, B. Mou, K. Li, P. Chiang, D. Wang, S. Lin, W. Tse, J. Raman Spectrosc. **32**, 53 (2001).

[14] A. R. Schmidt, S. Jancke, E. E. Lindquist, E. Ragazzi, G. Roghi, P. C. Nascimbene, K. Schmidt, T. Wappler, D. A. Grimaldi, PNAS **109**, 14796 (2012).

[15] M. Feist, I. Lamprecht, F. Müller, Thermochim. Acta **458**, 162 (2007).

[16] G. López-Morales, R. Espinosa-Luna, C. Frausto-Reyes. Rev. Mex. Fis. **60**, 217 (2014).

[17] F. C. Alvira, T. Flores Reyes, L. Ponce Cabrera, L. Moreira Osorio, Z. Perez Baez, G. Vazquez Bautista, Appl. Opt. **54**, 4453 (2015).

[18] F. C. Alvira, G. M. Bilmes, T. Flores, L. Ponce, Appl. Spectrosc. **69**, 1205 (2015).

[19] G. Vítková, L. Prokeš, K. Novotný, P. Pořízka, J. Novotný, D. Všianský, L. Čelko, J. Kaiser, Spectrochim. Acta-B: Atom. Spectrosc. **101**, 191 (2014).

Table 3. Detailed description of the spectroscopic signal shown in Fig. 2.

Element	I (nm)	M. Yellow	Y. Baltic	F. Yellow	M. Honey	B. Honey	F. Honey
Ni I	231.7	x	-	-	x	-	-
Ni I	232	x	-	-	x	-	-
Si I	250.6	x	x	x	x	x	x
Mn I	279.8	-	x	-	-	x	-
Co I	358	-	-	-	x	-	-
Sr I	407.7	x	-	-	x	-	-
Co I	384.5	-	-	-	x	-	-
Co I	399.5	-	-	-	x	-	-
Si I	385.7	x	x	x	x	x	x
Ni I	385.8	x	-	-	-	x	-
Ca II	393.36	x	x	x	x	x	x
Al I	394.4	x	x	x	x	x	x
Al I	396.1	x	x	x	x	x	x
Ca II	396.84	x	x	x	x	x	x
Sr II	405	x					
Ca I	422.67	x	x	x	x	x	x
Ca I	430.25	x	x	x	x	x	x
Ca I	443.57	x	x	x	x	x	x
Ba II	455.4		x			x	
Ba II	493.4	-	x		-	x	
Hβ	486.1	x	x	x	x	x	x
N I	500.5	x	x	x	x	x	x
Ni I	508	x	-	-	-	x	-
Ni I	558.9	x	-	-	-	x	*
Fe I	567.9	x	x	x			x
Na I	588.99	x	-	-	x	-	-
Na I	589.59	x	-	-	x	-	-
N I	648.53	x	x			x	x
Hα	656.3	x	x	x	x	x	x
Li I	670.79	x				x	
N I	742.4		x	x	x	x	x
N I	744.2						x
N I	746.83		x	x	x	x	x
K II	766.49	x	x	x		x	
K I	769.89	x				x	
O I	777.2	x	x	x	x	x	x
Ni I	231.7	x	-	-	x	-	-
Ni I	232	x	-	-	x	-	-